Engineering Fracture Mechanics 276 (2022) 108933

Contents lists available at ScienceDirect

Engineering Fracture Mechanics

journal homepage: www.elsevier.com/locate/engfracmech

Comprehensive investigation of rock fracture behaviour in clay-rich rocks under the effect of temperature: Experimental study under three loading modes (I, I/II, II)

Mahmoud Alneasan [a], Abdel Kareem Alzo'ubi [b,*]

[a] Civil Engineering Department, Tishreen University, Latakia, Syria
[b] Civil Engineering Department, Abu Dhabi University, Al Ain, United Arab Emirates

ARTICLE INFO

Keywords:
Temperature
Mixed-mode loading I/II
Mudstone
Fracture toughness
Fracture envelope
Crack propagation speed
Crack acceleration

ABSTRACT

Rock fracture behaviour is a crucial aspect in many geological and engineering projects and can be affected by different environmental factors such as temperature, especially in projects where the rocks are exposed to a change in temperature such as geothermal energy, oil and gas exploitation, nuclear waste areas, etc. Therefore, this research aims to investigate the effect of temperature on rock fracture behaviour under four loading modes; pure mode I, pure mode II, and two mixed-mode loadings I/II in SCB specimens of clay-rich rocks (mudstone). Thirty-six SCB specimens were prepared and tested under three temperatures (Ambient temperature (AT), 250 and 500 °C), and some important parameters such as fracture toughness, fracture envelope, crack propagation speed, and crack acceleration were measured and discussed as a function of temperature. The main results concluded that due to the gradual loss of water from the structure of high clay content in the mudstone during thermal treatment, the behavior of mudstone gradually changed from ductile to brittle behaviour, and as a result, fracture toughness and crack propagation speed increased significantly. In addition, our results showed that the area under the fracture envelope which represents fracture resistance to growth under mixed-mode loading increased by 1.86 and 2.68 orders in magnitude after thermal treatment at temperatures of 250 and 500 °C, respectively. Under the four loading mode mixities, fracture grows through three main stages, high acceleration (0–5 mm), high deceleration (5–10 mm), and low deceleration (10–15 mm) stages. Crack propagation speed and crack acceleration depend strongly on the mode mixity ratio (K_{II}/K_I) and it increased by changing the loading mode from pure mode I to mixed mode loading I/II and pure mode II.

1. Introduction

Surfaces of weakness such as micro cracks, cracks, joints, faults, etc. are abundant in the rock mass and are exposed to many environmental factors that affect their properties and extension [10]. Temperature is one of the most important factors that affect intact rock properties due to thermal stresses. Moreover, it has many practical applications in the field of rock mechanics such as the disposal of highly radioactive nuclear waste, exploitation of geothermal resources, coal bed methane displacement and exploitation, hydraulic fracturing, and stability of roadways, embankments, and slopes [11,15,39,49].

* Corresponding author.
E-mail addresses: mahmoud.alneasan@tishreen.edu.sy (M. Alneasan), abdel.alzoubi@adu.ac.ae (A.K. Alzo'ubi).

https://doi.org/10.1016/j.engfracmech.2022.108933
Received 30 June 2022; Received in revised form 5 November 2022; Accepted 7 November 2022
Available online 12 November 2022

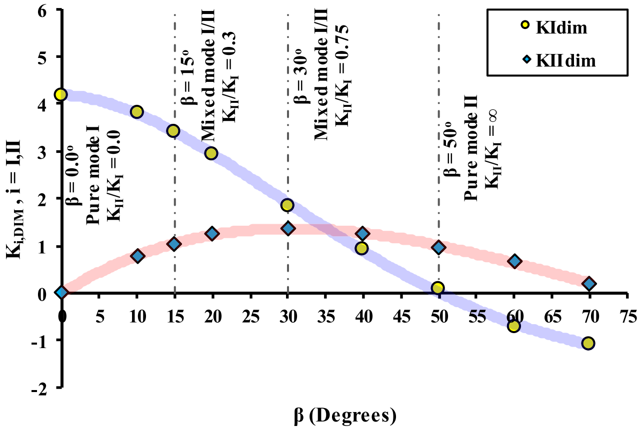

Fig. 1. Stress intensity factors are calculated depending on the DDM as a function of the notch inclination angel.

The behavior of fractures by considering the effect of temperature has been studied by many researchers under different loading modes, pure mode I, mixed-mode loading I/II, and pure mode II. Most studies related to temperature effects in the field of rock fracture mechanics focused on pure mode I, especially the effect of temperature on the pure mode I fracture toughness [18,28,30;43,47]. However, some of the studies were conducted under pure mode II [19,26,45]. Depending on the rock type and the temperature to which rock samples are exposed, previous studies indicated negative or positive effects of thermal treatment on rock properties, such as increasing or decreasing fracture toughness. Studies related to temperature effects on fracture properties under three loading modes together are rare compared to those under pure mode I or pure mode II. Yin et al. [46] investigated mixed-mode tensile fracturing in thermally treated notched Brazilian disks of granite at temperatures of 25, 100, 200, 400, 600, and 800 °C. In their study, four loading mode mixities; pure mode I, pure mode II, and two mixed-mode loadings; were considered. They showed that the brittleness and the mixed-mode fracture toughness are significantly affected by thermal treatment. Feng et al. [20] studied the effect of temperature on the thermally treated SCB specimens of sandstones under mixed-mode loading and at temperatures from about 20 to 600 °C. They showed that for T $>$ 500 °C, the mixed-mode (I/II) and mode II fracture behaviour are significantly affected by thermal treatment. The impact of temperature on the mixed-mode fracture toughness is similar to that on pure mode I fracture toughness. Kang et al. [29] investigated experimentally fracture behaviour in SCB specimens of granite under three modes mixities (pure mode I, mixed-mode I/II, and pure mode II) after thermal treatment at temperatures of 20, 300, 600, and 900 °C. They concluded that as the temperature increased the tensile strength decreased. and the fracture toughness of SCB specimens rapidly decreased at T $<$ 600 °C, while it slowly decreased for treated specimens at T $>$ 600 °C. Dehghani and Faramarzi [17] studied experimentally the effect of mode mixity and freezing and thermal cyclic loading on fracture toughness and crack initiation in SCB specimens of marble. They changed the temperature between −30 and 160 °C and they showed that the crack initiation angles under mixed-mode I/II and mode II conditions were 58° and 78°, respectively. In addition, the mode I fracture toughness decreased under the Freezing-Cooling-Heating condition. In a recent study, Wu et al. [42] study numerically mixed-mode fracture characteristics of granite using the extended finite element method, which depends on the CZM (Cohesive Zone Model). The developed numerical model can successfully predict fracture trajectory and fracture loads in notched Brazilian disks of granite under mixed-mode loading and temperatures between 25 and 600 °C. Su et al. [35] showed depending on experimental tests on thermally treated CSTBD specimens of granite under dynamic loading that the fracture toughness decreases gradually as the mixed coefficient increases. Dynamic fracture toughness decreased slightly for T between 25 and 400 °C and sharply for T between 400 and 800 °C.

As observed in the literature the investigations under mixed-mode loading I/II need to be further expanded by studying topics that have not been sufficiently highlighted such as the effect of temperature on the fracture envelope and the dependence of fracture toughness on the temperature in clay rick rocks or investigating new topics such as the effect of temperature on the crack propagation speed under three loading modes (I, I/II and II). In this study, we investigated fracture toughness, fracture envelope, crack propagation speed and crack acceleration in SCB specimens of mudstone (clay-rich rock) under three temperatures (ambient temperature, 250 and 500 °C) and four loading modes mixities (pure mode I, pure mode II and tow mixed mode loadings I/II.

2. Numerical modelling

Three points bending tests on the semicircular specimens were simulated depending on the displacement discontinuity method (DDM). This simulation was done before the experimental procedure to determine the geometric properties of the semicircular specimen in terms of the radius (R), notch length (a), notch inclination angle (β), and the spacing between the two supports (2S) during the test. Depending on the geometric properties of the SCB specimen, especially (a/R, β, and S/R), different loading modes can be obtained. A Two-dimensional crack propagation code (TDCPC) was previously developed by Alneasan et al. [8] to predict stress intensity factors and crack propagation path in SCB specimens for a/R = 0.3 and S/R = 0.43. This code was verified in different studies and was used to study different problems for crack initiation and propagation in brittle rocks under static and dynamic loads [5,6;7].

Table 1
Physical and mechanical properties of the mudstone used in this study.

Property	Density	BTS	UCS	P-wave	S-wave	R-wave	E	ν
Magnitude	2.6	3.2	108.7	4719	2668	2452	44	0.3
Unit	gr/Cm^3	MPa	MPa	m/s	m/s	m/s	GPa	–

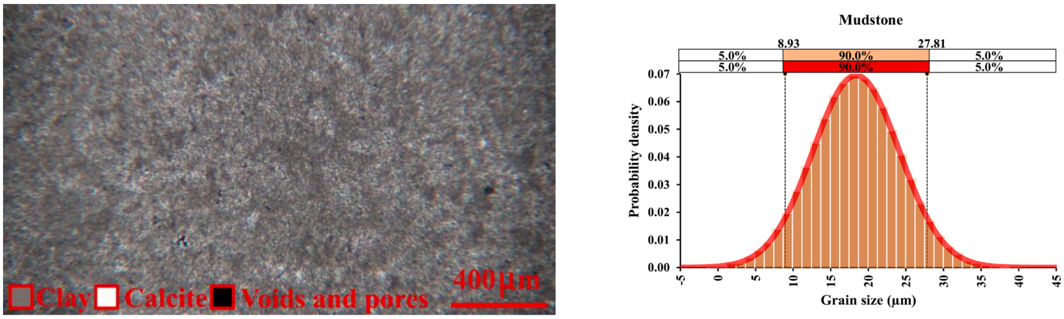

(a) (b)

Fig. 2. (a) Microscopic thin section under the microscope (lens 20X), (b) grain size distribution.

(a)

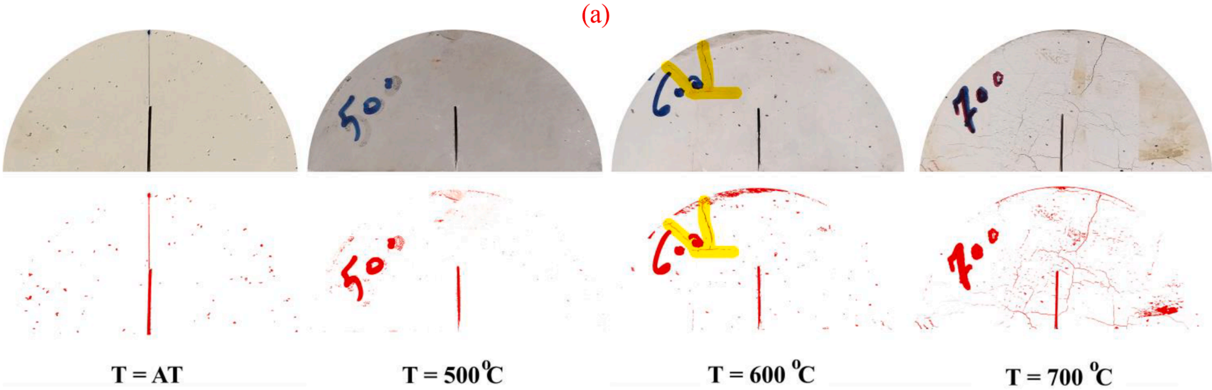

(a)

Fig. 3. (a) The furnace used in this study to hat SCB specimens, (b) SCB specimens after thermal treatment at 500, 600, and 700 °C ompared to the ambient temperature (AT).

Depending on the TDCPC, stress intensity factors were computed as a function of the β for R = 50 mm, a = 25 mm (a/R = 0.5), and 2S = 60 mm (S/R = 0.6), and the results are shown in Fig. 1. This figure shows that for β = 0.0 and 50°, the notch tip is subjected to pure tension and pure shear stress and the SCB specimen is under pure mode I and pure mode II, respectively. For 0.0 < β < 50°, the notch tip is subjected to tensile and shear stress at the same time and the SCB specimen is under mixed-mode loading. Based on that, four values of the β = 0.0, 15, 30, and 50° were adopted in this study to cover the cases of pure mode I, mixed-mode loading I/II, and pure mode II.

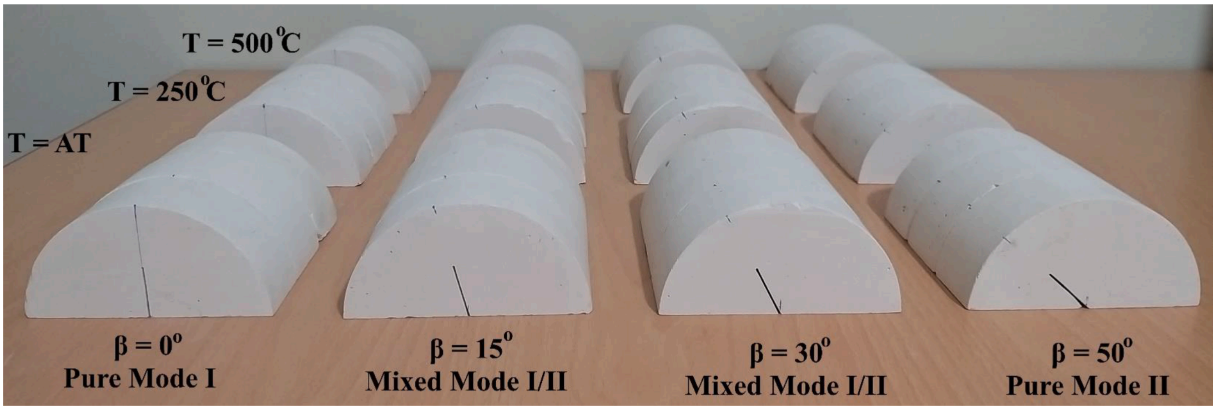

Fig. 4. The SCB specimens prepared in this study to be tested under three loading modes.

3. Experimental procedure

The experimental work of this paper consists of four parts; determining the rock type, the thermal treatment, preparation of the SCB specimens, and crack propagation speed and loading system.

3.1. Determination of the rock type

This study investigates the effect of loading mode and thermal treatment temperature on the fracture behaviour in clay-rich rocks that have a high affinity for water. Therefore, mudstone was chosen in this study due to its high clay content. A microscopic thin section of this mudstone was taken and several experiments were conducted on this rock type. These experiments included Brazilian tensile strength (BTS), uniaxial compressive strength (UCS), sound wave velocities that include P-wave, S-wave, and R-wave velocity, Young modulus, and Poisson's ratio of the material. The physical and mechanical properties of the mudstone used in this study are summarized in Table 1. The microscopic thin section with grain size distribution is shown in Fig. 2. The predominant color in this figure is gray, which indicates high clay content. Depending on the analysis of grayscale, white, and black using the Image J program [1], the mudstone used in this study consists of 90% clay minerals, 8% calcite, and 2% voids and pores. Fig. 2-b shows that the mudstone consists of very fine grains of clay and calcite. It also shows that 90% of the grains have a maximum diameter between 8.93 and 27.81 μm.

3.2. Thermal treatment

In the beginning, five SCB specimens of the mudstone were prepared to be thermally treated under temperatures of 100, 250, 500, 600, and 700 °C. The furnace used for heating rock samples in this study is shown in Fig. 3-a. The maximum temperature that can be obtained using this furnace is 1200 at an increment of 4.2 °C per minute. Each sample was exposed to thermal treatment for 24 h in the furnace, where the temperature gradually increased at a rate of 4.2 °C/min from ambient temperature to the desired temperature. After 24 h, rock samples were gradually cooled to the ambient temperature. After thermal treatment and cooling, the growth of thermal cracks on the surface of each sample was monitored with the naked eye. SCB specimens after thermal treatment at 500, 600, and 700 °C with the specimen under ambient temperature are shown in Fig. 3-b. The thermal cracks and defects on the surface of SCB specimens are shown in red color. For temperatures, less than 600 °C, such as T = 500 °C in Fig. 3-b, no thermal cracks were observed on the surface of the specimen. However, for T = 600 °C, three intersecting cracks were observed on the upper part of the sample surface as shown in Fig. 3-b. For T = 700 °C, a network of thermal cracks appeared on the surface of the sample. Therefore, the temperature of 500 °C was adopted as the maximum temperature for treating the original samples of this study. Which is approximately the maximum temperature at which no thermal cracks were observed on the surface of the SCB specimens.

3.3. Preparation of SCB specimens

To investigate the effect of thermal treatment on the mechanical properties of clay-rich rocks such as mudstone, experimental conditions should be determined and a sample type should be selected to achieve the goal of this study. The mechanical properties of fractures can be experimentally studied using different types of pre-notched specimens, however, semi-circular specimens were selected for ease of preparation and testing under different loading modes [41]. As shown in the following paragraph, the required loading mode can be obtained by controlling three parameters; the notch length (a), the distance (2S) between the lower supports under the sample, and the notch inclination angle (β). Moreover, to study the effect of temperature on the mudstone, the SCB specimens were thermally treated in the furnace at different temperatures. Accordingly, the displacement-load curves, fracture toughness, fracture envelope, crack propagation speed, and crack acceleration obtained as a function of thermal treatment temperature and

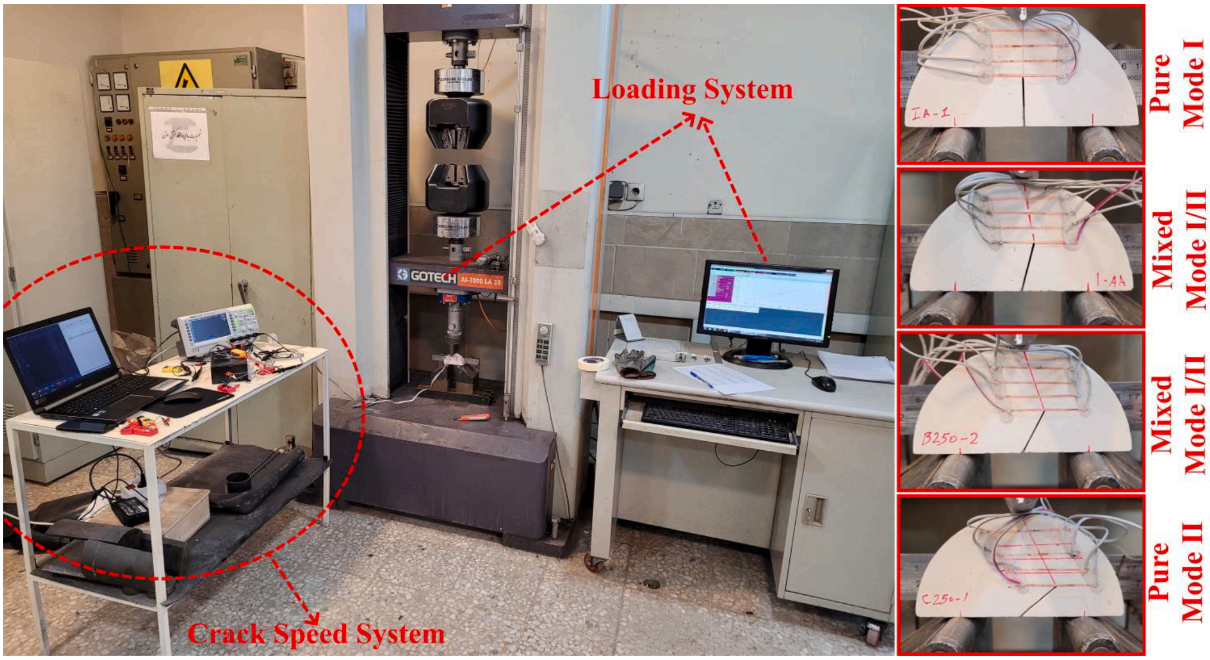

Fig. 5. Loading device and crack propagation speed system.

loading mode.

Depending on the numerical simulation of the three points bending test and on the dimensionless stress intensity factors as a function of the β shown in Fig. 1, four sample configurations of SCB specimens were prepared from mudstone to cover the three loading modes in this study. As shown in Fig. 4, the first sample configuration has a zero notch inclination angle (β = 0.0) to obtain pure mode I with ($K_I \neq 0.0$ and $K_{II} = 0.0$). The second and third configurations have a notch with an inclination angle of 15° and 30°to cover mixed-mode loading with ($K_{II}/K_I = 0.3$ and 0.75), respectively. The fourth configuration has a notch with an inclination angle of 50° to get pure mode II with ($K_I = 0.0$ and $K_{II} \neq 0.0$). Note that the dimensions of the SCB specimens were the same as the ones used in the numerical simulation; R = 50 mm, a = 25 mm (a/R = 0.5), and 2S = 60 mm (S/R = 0.6), T = 35 mm (T/R = 0.7). Moreover, the SCB specimens, prepared in this study, were tested under three temperatures; T_1 = AT, T_2 = 250, and T_3 = 500 °C, and each test was repeated three times. Therefore, the number of SCB specimens prepared in this study was 4 × 3 × 3 = 36 specimens as shown in Fig. 5.

3.4. Crack propagation speed system

Crack propagation speed under three loading modes was measured by using a special electrical circuit which was previously developed by Alneasan and Behnia [5] to study the effect of strain rate on the crack propagation speed in hornfels rock under three loading modes. The loading device and crack propagation speed system used in this study are shown in Fig. 5. The electrical circuit for measuring crack propagation speed consists of four conductive copper tapes, four power supplies (3 V), a digital oscilloscope with four channels, and conductive wires to connect the electrical circuit. The surface of the SCB specimen is well-smoothed and polished to ensure complete contact between the conductive tapes and the rock sample. The first tape is glued directly at the notch tip, so this tape will cut off at the moment of crack initiation at the tip of the joint. The other three tapes are glued at a spacing of 5 mm between each other. These tapes are connected to the power supply and digital oscilloscope by using conductive wires (Fig. 5). The oscilloscope is set by using trigger mode to detect the signal when the electrical circuit is cut off. Depending on this signal, the cut off time of each copper tape is determined. It must be noted that the conductive tapes -are glued to the sample and they will cut off whenever the fracture passes under them. Crack propagation speed between every-two successive tapes is calculated depending on the cut off time and the length of fracture between them. Therefore, we have four values for the crack propagation speed, the first speed is c_1 and equals zero. c_1 represents the crack velocity just before crack growth. The second speed is c_2 and corresponds to the average crack propagation speed between the first and second tapes. The third (c_3) and fourth (c_4) speeds represent the average value of crack propagation speed between the second and third, third, and fourth copper tapes, respectively.

4. Results and discussion

The effect of thermal treatment on the fracture toughness and crack propagation speed under three loading modes in clay-rick rocks such as mudstone is investigated in this study. The notch inclination is varied to produce different loading modes to investigate the effect of temperature treatment on the fracture toughness, fracturing speed, and acceleration as discussed below. Note that all relevant

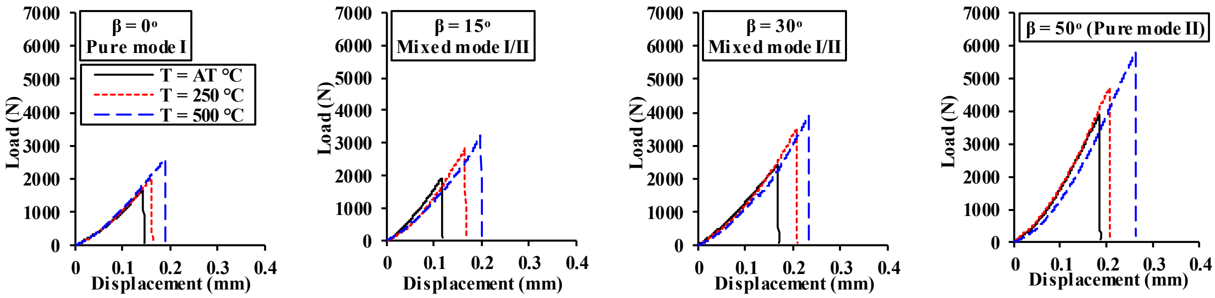

Fig. 6. Displacement – load curves as a function of the temperature and notch inclination angle.

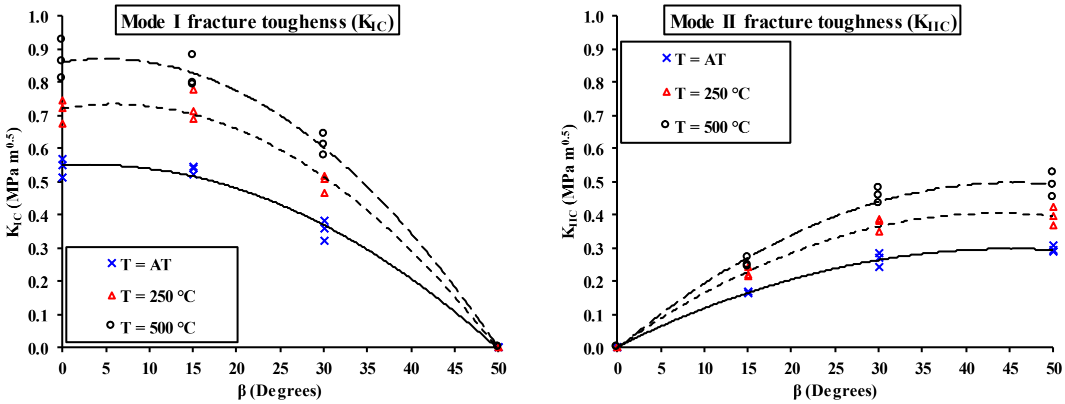

Fig. 7. Mode I and II fracture toughness as a function of the temperature and notch inclination angle.

experimental data used in this work are summarized in Table 3 in appendix I.

4.1. Fracture toughness

The variation of β in the SCB specimens determines the mode mixity ratio (K_{II}/K_I) in each tested sample. To calculate K_{IC} and K_{IIC} equation (1) was used as a function of β, where P_{cr} is the peak of the load–displacement curve, R, T, and (a) are the radius, thickness, and notch length, respectively, $K_{i,Dim}$ (i = I, II) are dimensionless stress intensity factors and can be obtained from Fig. 1.

$$K_{ic} = \frac{P_{cr}}{2RT} K_{i,Dim} \sqrt{\pi a}\ (i = I, II) \tag{1}$$

The experimental results show that by increasing β and the T, the maximum load at failure increased and the area under the curves increased as well. The load- Displacement curves of SCB specimens as a function of temperature (T) and β are shown in Fig. 6. To make it easier to read the curves, one curve for each T and β is shown in this figure. The increase in the area under the load–displacement curve shows that the rock was able to store more energy before a fracture initiation. Moreover, the clay-rich material gain strength as a result of thermal treatment. It should be noted that, after thermal treatment at temperatures of 250 and 500 °C, this displacement at the peak load increases in comparison with the displacement at failure at the ambient temperature. For β = 0.0, 15, and 30°, the displacement at failure ranges between 0.1 and 0.25 mm, while under β = 50° (pure mode II), the range of displacement at failure increases to 0.18 – 0.43 mm. These results show that tensile fracturing occurs at a lower load and lower displacement once compared to the shear mode of failure. As we move from tension to shear the same trend occurred as shown in the figure.

Fig. 7 shows Mode I and II fracture toughness as a function of T and β. As expected, by increasing the β, the notch tip gradually moves from pure mode I to mixed mode loading I/II and pure mode II. The most notable result is that by increasing the temperature from AT to 250 and 500 °C, fracture toughness under all βs significantly increases. For example, increasing the temperature from ambient temperature to 500 °C, K_{IC} under β = 0.0, 15, and 30° increases by 59%, 53%, and 72%, respectively. The same trend was also observed for K_{IIC} as shown in the figure, for, β = 15, 30, and 50° K_{IIC} increases by 54%, 73%, and 66%, respectively. It can be noted that K_{IC} and K_{IIC} have almost the same rate of increase after thermal treatment. In addition, it can be noted that for all βs and all temperatures, K_{IIC} is less than K_{IC}.

Our results focused on the regime for the effect of temperature on the fracture toughness of mudstone under four mode mixites, and the direct proportion between temperature and fracture toughness. The effect of temperature on the fracture toughness of rock mainly depends on the mineralogical composition of the rock and it was investigated by many researchers on different rock types, especially

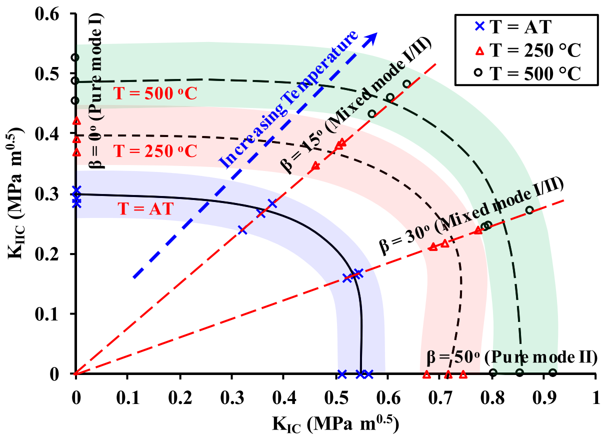

Fig. 8. Experimental results for fracture envelopes of the mudstone after thermal treatment.

the effect of temperature on the K_{IC}. Feng et al. [20] investigated the effect of temperature on the mixed-mode I/II and mode II fracture toughness in sandstone and concluded that $K_{I/IIC}$ and K_{IIC} increase and decrease slowly for 20 < T < 100 and 100 < T < 500 oC, respectively. For 100 < T < 500 °C, fracture toughness under mixed-mode loading and pure mode II decreases sharply. Zhang et al. [50] noticed a decrease in dynamic fracture toughness under pure mode I in gabbro and marble for T between 20 and 600 °C. Funatsu et al. [25] studied the effect of temperature between 25 and 200 °C on the K_{IC} in sandstone and tuff and showed that for tuff and T between 25 and 75 °C, K_{IC} decreased with increasing the temperature and then started to increase for T > 75 °C. While for the sandstone, K_{IC} was approximately constant for T between 25 and 125 °C and then it increased for T > 125 °C. Al-Shayea et al. [2] concluded that the K_{IC} of limestone increased by about 25% by increasing the temperature from 27 to 116 °C. Balme et al. [14] investigated the effect of thermal treatment on the basalt and showed a marked increase of the K_{IC} at around T = 150 °C. While for Etnean or Vesuvian basalt, the K_{IC} was not greatly affected by increasing the temperature. Zuo et al. [51] showed three regimes for the effect of temperature on the K_{IC}, K_{IC} decreased slightly for T between 25 and 100 °C, then it increased significantly for 100 < T < 125 °C, and then gradually decreased by increasing the temperature from 125 to 600 °C. It can be seen that for most rock types shown in this section, most researchers indicated either a decrease in fracture toughness after thermal treatment or two regimes for the effect of temperature on fracture toughness. However, our experiments on the mudstone showed a significant improvement in fracture toughness with increasing temperature. As will be shown in Section 4.5, because of the high clay content in the mudstone and the clay's sensitivity to water, clay minerals gradually lose water during thermal treatment, which increases the rigidity of the mudstone and thus improves the strength properties of the rock.

4.2. Fracture envelope

The fracture envelope is important to determine the conditions for crack growth under mixed-mode loading [41]. Under pure mode I (β = 0.0 in SCB specimens) and pure mode II (β = 50°), the notch tip will initiate once K_I and K_{II} reach K_{IC} and K_{IIC} of the material, respectively. Under mixed-mode loading, the notch tip is subjected to tensile ($\sigma_n \rightarrow K_I$) and shear ($\tau_n \rightarrow K_{II}$) stresses. Therefore, both mode I and II stress intensity factors (K_I, K_{II}) contribute in different proportions to the fracturing process. Fracture envelope in rocks and other materials was investigated by many researchers under the effect of different factors, such as strain rate. These factors may cause increasing the area beneath the fracture envelope. i.e., the material resistance for crack growth under mixed-mode loading. On the other hand, when the studied factors cause the downward movement of the fracture envelope the opposite will occur. Aliha et al. [3] concluded that by increasing the displacement rate in PMMA, the area under the fracture envelope decreases and the material resistance for crack growth under mixed-mode II decreases. While Alneasan and Behnia [6] showed that by increasing the strain rate from 10^{-4} to 10^{-2} S^{-1}, the area under the fracture envelope increased and the material resistance for crack growth under mixed-mode loading increased by about 35%. Dehghani and Faramarzi [17] investigated the effect of freezing and thermal cyclic loading on the fracture toughness and fracture envelope in marble, they indicated that the material resistance for crack growth decreases by increasing the temperature. The same result was observed by Meng et al. [33] in sandstone.

In our study, experimental results for fracture envelopes of the mudstone after thermal treatment at temperatures of AT, 250, and 500 °C are shown in Fig. 8. The most important result that can be noted in this figure is that by increasing the temperature, the fracture envelope moves up and to the right i.e., the area under the curve increases, and the fracture resistance to grow under mixed-mode loading I/II in the mudstone increases. The area under the first fracture envelope for T = AT is 0.152 MPa^2 m and it increases by 1.86 and 2.68 orders of magnitude after thermal treatment at temperatures of 250 and 500 °C, respectively.

4.3. Crack propagation speed

To analyze stress and strain fields in the vicinity of the crack tip under quasi-static and dynamic loads, the crack propagation speed

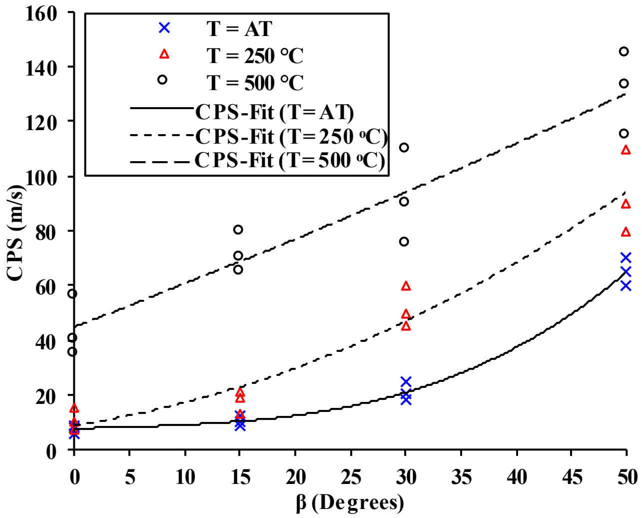

Fig. 9. Crack tip speed between the first two copper tapes versus notch inclination angle and temperature.

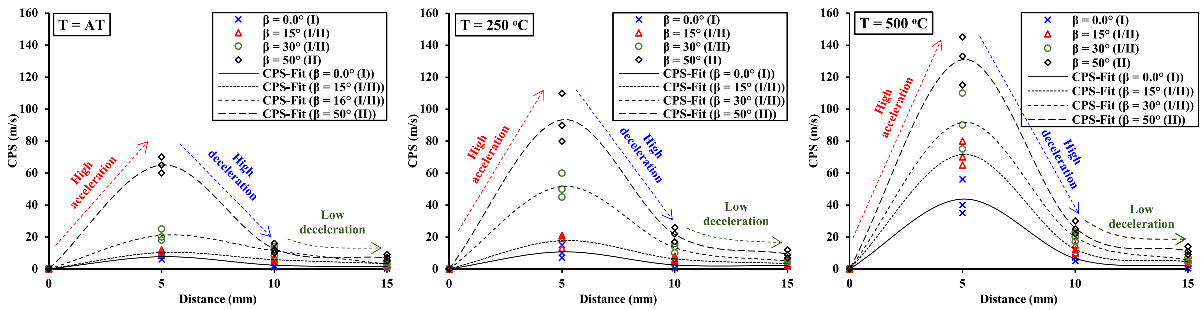

Fig. 10. Crack propagation speed versus the distance between copper tapes under ambient temperature, 250 and 500 °C.

must be known. Freund [24] showed that asymptotic stress and strain field around a moving crack tip under any loading mode are functions of the crack tip velocity, and their magnitudes increase by increasing the crack propagation speed. In addition, dynamic stress intensity factors for a moving crack tip are functions of the crack propagation speed. The ratio between dynamic to static stress intensity factors (K_d/K_s) under pure mode I [48] and pure mode II [23] decreases from 1 for ($c = 0.0$) to 0.0 for ($c = c_r$). Where c_r is the Rayleigh wave speed which generally represents the maximum crack propagation speed in different media. Liu et al. [32] investigated the effect of the elastic modulus of four brittle materials (black sandstone, red sandstone, green sandstone, and BMMA) on the crack propagation speed and showed that the crack tip speed is directly proportional to the elastic modulus. Recently, Alneasan and Behnia [4] investigated the effect of the grain size of granite on the crack propagation speed and concluded that by increasing grain size, the crack propagation speed decreases. Moreover, Alneasan and Behnia [5] also conducted a comprehensive study on the effect of strain rate and loading mode on the crack propagation speed in hornfels rock. They concluded that the crack propagation speed under pure mode II is larger than that under pure mode I and mixed-mode loading I/II. In addition, they showed that the crack tip speed under dynamic loads (drop weight machine) is significantly greater than that under quasi-static strain rate (servo-hydraulic machine). [12,13,31,36,40], showed that the crack propagation speed is not constant along the fracture trajectory, and the crack can accelerate or decelerate along its path.

In this study, we investigated the effect of thermal treatment at three temperatures (AT, 250, and 500 °C) on the crack propagation speed. We tested that under three loading modes (I, I/II, and II) in SCB mudstone specimens. Fig. 9 shows the crack propagation speed between the first two copper tapes as a function of β and temperature. The results clearly show that under ambient temperature, the average value of the crack propagation speed increases from 7.7 to 65 m/s as β increases from 0.0 to 50°. It is also evident that the crack speed increases with increasing temperature. So, the crack propagation speed is directly proportional to the β and T. For example, under pure mode I ($\beta = 0.0°$), by increasing the T from AT to 500 °C, the crack propagation speed increases from 7.7 to 43.3 m/s. While under pure mode II ($\beta = 50°$), the crack propagation speed increases from 65 to 131 m/s when the T increases from AT to 500 °C.

Table 2
Average values of crack acceleration and deceleration between each two successive copper tapes.

$\dot{c}$ (m/s^2)	**β = 0.0 (Pure mode I)**			**β = 15° (Mixed-mode I/II)**			**β = 30° (Mixed-mode I/II)**			**β = 50° (Pure mode II)**		
	AT	**250**	**500**	**AT**	**250**	**500**	**AT**	**250**	**500**	**AT**	**250**	**500 °C**
0–5 (mm)	6×10^3	1×10^4	2×10^5	1×10^4	3×10^4	5×10^5	4×10^4	2×10^5	7×10^5	3×10^5	6×10^5	1×10^6
5–10	-4×10^3	-1×10^4	-2×10^5	-6×10^3	-2×10^4	-4×10^5	-3×10^4	-2×10^5	-7×10^5	-3×10^5	-6×10^5	-1×10^6
10–15	-3×10^2	-3×10^2	-3×10^3	-2×10^3	-2×10^3	-1×10^4	-1×10^4	-1×10^4	-3×10^5	-8×10^3	-3×10^4	-4×10^4

4.4. Crack acceleration

To investigate the crack propagation acceleration, the crack propagation speed was measured in this study by using four copper tapes. Each value of these speeds represents the average crack propagation speed between every-two successive tapes. Depending on changes in the crack tip speed vs the time, the crack accelerating or decelerating can be calculated. Fig. 10 shows the crack propagation speed versus time, this figure roughly determines the crack acceleration or deceleration points. This figure shows three trends in the crack tip speed along the distance between the notch tip and final copper tape (0 to 15 mm). For the first part (0–5 mm) high acceleration stage was observed such that the, crack propagation speed greatly increases and the fracture tip grows through high acceleration. The crack propagation speed reaches its maximum value at this range (0–5 mm). For the second part (5–10 mm) a high deceleration stage was observed and the crack propagation speed significantly decreases and the fracture tip grows through high deceleration. For the third part (10–15 mm), a low deceleration stage was noticed such that the fracture tip grows at a low deceleration or at an almost constant speed. Due to the large changes in the crack tip speed within the first and second regimes (0–10 mm), it can be said that the distance between the notch tip and the third copper tape corresponds to an unstable crack propagation stage. This stage is about 40% of the distance between the notch tip and the top of the SCB specimen (25 mm). Due to the low deceleration or almost constant speed in the third stage (10–15 mm), the distance between the third and fourth copper tapes corresponds to a stable crack propagation stage which is about 20% of the distance between the notch tip and the top of the SCB specimen.

The behavior of crack acceleration and deceleration was observed at all tested samples and temperatures to a different extent, which indicates that the temperature and the inclination angle of the notch have a great effect on the fracturing behavior with time and distance. Fig. 10 shows that by increasing T or β, the magnitudes of crack acceleration and deceleration increase and change qualitatively. Therefore, the quantitative changes in crack acceleration and deceleration are summarized in Table 2, the positive and negative values in this table indicate crack acceleration and deceleration, respectively.

4.5. Explanation of the observed results

The laboratory results showed one trend for the effect of temperature on fracture toughness, fracture envelopes, crack propagation speed, crack acceleration, and deceleration. By increasing the T, all of the previous parameters increase. Taking into account the effect of T on the fracture toughness of other rock types shown in Section 4.1, It can be noted that most researchers noticed two regimes for the effect of temperature on fracture toughness. The most common observed regime is an increase in the fracture toughness with increasing the temperature up to a certain limit, and then a decrease in the fracture toughness. This regime can be observed in granite and rocks that have a low content of clay minerals and high content of calcium compounds such as limestone, siltstone, and sandstone.

For granite, the behavior of this rock type after thermal treatment is highly affected by the growth of thermal microcracks. Su et al. [35], Yin et al. [44] investigated the effect of thermal cracking on thermally treated samples of granite by using the scanning electronic microscopy (SEM) method and concluded that, by increasing the temperature to a certain limit (T_{cr}), new thermal microcracks grow and are randomly distributed in the rock sample. The random distribution of these microcracks around the notch tip obstructs the notch tip growth process. Therefore, these thermal microcracks need more energy to grow and connect to form weak surfaces in the rock sample that contribute to the fracture process. Increasing the energy required for the growth and coalescence of thermal microcracks causes an increase in fracture toughness. When the granite is thermally treated above a certain limit T_{cr}, thermal microcracks grow and coalesce with each other under the effect of temperature and form relatively large weak surfaces in the rock sample. This in turn causes a weakening in the fracture toughness under the influence of external mechanical loads.

For the rocks that have a low content of clay minerals and high content of calcium compounds such as limestone, the increase of temperature to a certain limit T_{cr} leads to the expulsion of water from clay layers through dehydration and dihydroxylation processes [2,25]. This leads to an increase in the strength of these rocks and a gradual transformation in their behavior from ductile to brittle behavior. By increasing the temperature above a certain limit T_{cr}, the role of drying clay minerals ends in increasing the strength of the rock sample, and then the strength decreases due to the decomposition of calcium compounds with increasing the temperature.

For the mudstone used in this study, as shown in Section 3.1, this rock type has a high clay content (about 90%) and a low content of calcite (about 8%). Therefore, clay minerals are a major influencing factor on the strength properties of this rock type under thermal treatment. Drying of clay minerals during the thermal treatment of mudstone takes place through two main stages [38]. The first stage is the dehydration stage, which occurs at temperatures between 100 and 200 °C. The adsorbed, pore, and interlayer water is removed from clay minerals during this stage. The second stage is the dihydroxylation process, which occurs at temperatures between 500 and 1000 °C. This stage includes the ejection of hydroxyl ions from the crystal structure of the clay minerals, causing complete drying of clay minerals and generating localized tensile stress inside the rock sample [16,34], which in turn leads to the growth of thermal cracks which were observed in Fig. 3-b at a temperature of 600 and 700 °C. Therefore, it can be concluded that with thermal treatment of the mudstone to a temperature less than $T_{cr} = 500$ °C, the water between clay layers dries up without visible thermal cracks on the rock surface, and the rock behaviour transforms gradually from ductile to brittle, and the fracture toughness significantly increases with increasing the temperature. Feng et al. [21]; Feng et al. [22] investigated the effect of thermal treatment for temperature up to 400 °C on the elastic modulus of triaxially stressed mudstone. They concluded that the observed changes in elastic modulus were due to the effect of thermal cracking, thermal expansion, water loss, and reconstruction of clay minerals. Thermal expansion enhanced mudstone properties by opposing deformation due to the applied compression. Mineral structure changes also have a significant impact on the elastic modulus due to the loss of water within the structure and its consequent reconstruction at high temperatures. In addition, some researchers discussed some hypotheses for the effect of temperature on clay minerals in terms of the thickness of the diffuse double layer. For example, Houhou et al. [27] investigated the effect of thermal loading on the microstructure of the compacted clays and concluded that by increasing the temperature, the thickness of the diffuse double layer decreases. Therefore, clay minerals get closer together and the contact between them increases, which in turn causes an increase in the density and strength properties of clay [37].

As for the effect of temperature on the crack propagation speed, crack acceleration, and deceleration, as mentioned previously, by increasing the temperature, clay minerals gradually lose the water between their layers, and the mudstone hardens and its behavior changes from ductile to brittle. Our previous experiments on cores of mudstone under uniaxial compressive stress by using vertical and horizontal strain gauges to measure elastic modulus and Poisson's ratio showed that by increasing the temperature from ambient temperature to 250 and 500 °C, the elastic modulus increased from 42.7 to 47.1 and 49.4 MPa, and the Poisson's ratio decreased from 0.377 to 0.335 and 0.303, respectively, [9]. The increase of elastic modulus and decrease of Poisson's ratio demonstrates the aforementioned transformation in material behaviour from ductile to brittle. Therefore, the crack propagation speed increased with increasing the temperature of thermal treatment in the mudstone. In addition, it was noted that by increasing the β from 0.0 to 50°, the crack propagation speed increases. Taking into account displacement – load curves in Fig. 6, by increasing the β, the area under displacement – load curves increases. Therefore, the SCB specimen stores more energy before the fracturing instant when the loading mode changes from pure mode I to mixed mode loading and pure mode II. Accordingly, increasing the amount of energy stored in the rock sample causes it to be released faster at the instant of fracture, and thus the fracture grows more quickly.

Since temperature is one of the most important environmental factors that influence the behavior of rock mass in many regions of the earth's crust that are exposed to varying thermal effects. The results of the current study are of great importance to be used in civil, mechanical, geological, and geophysical fields to predict fracture initiation and propagation in clay-rich rocks such as mudstone under the effect of temperature. Particularly for engineering applications where the rock mass is exposed to different levels of temperature such as geothermal energy, hydraulic fracturing, slope stability in areas exposed to high temperatures and wildfires, and the disposal or safe storage of radioactive waste in underground cavities.

5. Conclusions

The effect of temperature on rock fracture behaviour in mudstone was investigated in this study under four mode mixities (pure mode I, pure mode II and two mixed-mode loadings I/II). Thirty-six SCB specimens were prepared and tested after thermal treatment at three temperatures of ambient temperature (AT), 250, and 500 °C. Fracture toughness and crack propagation speed were measured. In addition, the fracture envelope under mixed-mode loading I/II and crack acceleration were discussed in terms of the effect of temperature.

The results of the study mainly indicated an improvement in the fracture resistance properties and fracture speed with increasing temperature. This improvement is a result of some important factors that occur in the clay structure during thermal treatment. Gradual water loss from clay structure through dehydration and dihydroxylation process that cause the reconstruction of clay minerals gradually changes the behaviour of mudstone from ductile to brittle behavior. As a result, the fracture toughness and crack propagation speed significantly improved.

The results related to fracture toughness indicated that by increasing T from AT to 500 °C, K_{IC} under $\beta = 0.0$, 15, and 30° increased by 59%, 53% and 72%, respectively. While K_{IIC} under $\beta = 15$, 30, and 50° increased by 54%, 73% and 66%, respectively. The fracture envelope which represents fracture resistance to growth under mixed-mode loading is temperature dependent and the area under it increased by 1.86 and 2.68 orders of magnitude after thermal treatment at temperatures of 250 and 500 °C, respectively.

The results related to crack propagation speed indicated that by changing the loading mode from pure mode I ($\beta = 0.0°$) to mixed mode loading ($\beta = 15$ and 30°) and pure mode II ($\beta = 50°$), crack propagation speed increases due to the increase in energy stored in the rock sample which is rapidly released at the moment of fracture. According to the effect of temperature on the crack propagation speed and crack acceleration. These two parameters were directly proportional to the increase in temperature of thermal treatment. In addition, under four mode mixities, fracture grows through three main stages, high acceleration (0–5 mm), high deceleration (5–10 mm), and low deceleration (10–15 mm) stages.

CRediT authorship contribution statement

Mahmoud Alneasan: Visualization, Validation, Software, Methodology, Investigation, Formal analysis, Data curation, Conceptualization, Writing - original draft. **Abdel Kareem Alzo'ubi:** Visualization, Validation, Methodology, Formal analysis, Conceptualization, Funding acquisition, Writing – review & editing, Supervision, Resources, Project administration.

Declaration of Competing Interest

The authors declare that they have no known competing financial interests or personal relationships that could have appeared to influence the work reported in this paper.

Data availability

Data will be made available on request.

Acknowledgment

We would like to thank the ORSP at Abu Dhabi University for funding this project (19300529, 19300528). We also would like to extend our thanks to Azmoneh Foulad Consulting Engineers[1] for permission to use facilities in this company's rock mechanics lab under the supervision of Eng. Mohsen Aghababaei[2] and Eng. Behzad Nateghpour[3].

Appendix A

Table 3

Table 3
A summary of the relevant data used in the current paper.

β	$K_{I\text{-}dim}$	$K_{II\text{-}dim}$	Sample No	P_{cr} (N)	D_f (mm)	K_{IC} (MPa $m^{0.5}$)	K_{IIC} (MPa $m^{0.5}$)	CPS (m/s)
T = Ambient Temperature (AT)								
0	4.18	0.00	AT-0-1	1687.50	0.125	0.565	0.00	9
			AT-0-2	1528.29	0.164	0.512	0.00	8
			AT-0-3	1638.63	0.143	0.548	0.00	6
15	3.42	1.05	AT-15-1	1987.30	0.134	0.544	0.167	12
			AT-15-2	1961.60	0.137	0.537	0.165	10
			AT-15-3	1901.76	0.116	0.521	0.16	9
30	1.84	1.38	AT-30-1	2177.19	0.135	0.321	0.241	25
			AT-30-2	2418.86	0.168	0.378	0.284	20
			AT-30-3	2567.72	0.195	0.378	0.284	18
50	0.00	0.98	AT-50-1	3886.00	0.185	0.00	0.305	70
			AT-50-2	3623.00	0.246	0.00	0.291	65
			AT-50-3	3714.69	0.211	0.00	0.291	60
T = 250 °C								
β	**$K_{I\text{-}dim}$**	**$K_{II\text{-}dim}$**	**Sample No**	**P_{cr} (N)**	**D_f (mm)**	**K_{IC} (MPa $m^{0.5}$)**	**K_{IIC} (MPa $m^{0.5}$)**	**CPS (m/s)**
0	4.18	0.00	250-0-1	2144.95	0.227	0.718	0.00	15
			250-0-2	2016.40	0.161	0.675	0.00	10
			250-0-3	2225.66	0.197	0.745	0.00	7
15	3.42	1.05	250-15-1	2511.21	0.224	0.71	0.218	21
			250-15-2	2591.41	0.183	0.71	0.218	19
			250-15-3	2830.38	0.165	0.775	0.238	13
30	1.84	1.38	250-30-1	3430.92	0.222	0.505	0.379	60
			250-30-2	3487.00	0.208	0.514	0.385	50
			250-30-3	3139.01	0.242	0.462	0.347	45
50	0.00	0.98	250-50-1	5382.34	0.263	0.00	0.422	110
			250-50-2	4993.79	0.342	0.00	0.392	90
			250-50-3	4688.46	0.205	0.00	0.368	80
T = 500 °C								
β	**$K_{I\text{-}dim}$**	**$K_{II\text{-}dim}$**	**Sample No**	**P_{cr} (N)**	**D_f (mm)**	**K_{IC} (MPa $m^{0.5}$)**	**K_{IIC} (MPa $m^{0.5}$)**	**CPS (m/s)**
0	4.18	0.00	500-0-1	2754.55	0.221	0.922	0.00	56
			500-0-2	2408.52	0.247	0.806	0.00	40
			500-0-3	2561.32	0.189	0.857	0.00	35
15	3.42	1.05	500-15-1	2906.32	0.158	0.796	0.244	80
			500-15-2	3202.51	0.198	0.877	0.269	70
			500-15-3	2882.96	0.248	0.789	0.242	65
30	1.84	1.38	500-30-1	3895.02	0.233	0.574	0.43	110
			500-30-2	4129.02	0.199	0.608	0.456	90
			500-30-3	4338.28	0.248	0.639	0.479	75
50	0.00	0.98	500-50-1	6679.61	0.413	0.00	0.524	145
			500-50-2	5755.38	0.261	0.00	0.452	133
			500-50-3	6193.53	0.314	0.00	0.486	115

D_f: Displacement at failure

[1] https://en.azmouneh.com/.
[2] m.aghababaei@mi.iut.ac.ir.
[3] b.nateghpour@mi.iut.ac.ir.

References

[1] Abràmoff MD, Magalhães PJ, Ram SJ. Image processing with ImageJ Biophotonics international 2004;11:36–42.
[2] Al-Shayea N, Khan K, Abduljauwad S. Effects of confining pressure and temperature on mixed-mode (I–II) fracture toughness of a limestone rock. Int J Rock Mech Min 2000;37:629–43.
[3] Aliha M, Samareh-Mousavi S, Mirsayar M. Loading rate effect on mixed mode I/II brittle fracture behavior of PMMA using inclined cracked SBB specimen. Int J Solids Struct 2021;232:111177.
[4] Alneasan M, Behnia M. An experimental investigation on tensile fracturing of brittle rocks by considering the effect of grain size and mineralogical composition. Int J Rock Mech Min 2021;137:104570.
[5] Alneasan M, Behnia M. Strain rate effects on the crack propagation speed under different loading modes (I, II and I/II): Experimental investigations. Eng Fract Mech 2021;258:108118.
[6] Alneasan M, Behnia M. Analytical and Experimental Investigation on The Effect of Loading Rate on The Fracture Toughness and Fracture Envelope in Brittle Rocks. Theor Appl Fract Mech. 2022;103300.
[7] Alneasan M, Behnia M, Bagherpour R. Frictional crack initiation and propagation in rocks under compressive loading. Theor Appl Fract Mech 2018;97:189–203.
[8] Alneasan M, Behnia M, Bagherpour R. Analytical and numerical investigations of dynamic crack propagation in brittle rocks under mixed mode loading. Constr Build Mater 2019;222:544–55.
[9] Alzo'ubi AK, Alneasan M. Experimental study on the effect of thermal treatment on the mechanical properties of clay-rich rocks (mudstone). Results. Engineering 2022;100728.
[10] Alzo'ubi A. Numerical simulation of mechanical movement of layered rock slopes. ISRM International Symposium-8th Asian Rock Mechanics Symposium OnePetro 2014.
[11] Alzo'ubi A. State of the art, reconstruction of damaged zones: transitory stresses effect and factors controlling rock mass stability. GEOMATE Journal 2018;14: 35–43.
[12] Arakawa K, Mada T, Takahashi K. Correlations among dynamic stress intensity factor, crack velocity and acceleration in brittle fracture. Int J Fract 2000;105: 311–20.
[13] Arakawa K, Takahashi K. Relationships between fracture parameters and fracture surface roughness of brittle polymers. Int J Fract 1991;48:103–14.
[14] Balme M, Rocchi V, Jones C, Sammonds P, Meredith P, Boon S. Fracture toughness measurements on igneous rocks using a high-pressure, high-temperature rock fracture mechanics cell. J Volcanol Geoth Res 2004;132:159–72.
[15] Chen J, Jiang F. Designing multi-well layout for enhanced geothermal system to better exploit hot dry rock geothermal energy. Renewable Energy 2015;74: 37–48.
[16] Cultrone G, Rosua FJC. Growth of metastable phases during brick firing: Mineralogical and microtextural changes induced by the composition of the raw material and the presence of additives. Appl Clay Sci 2020;185:105419.
[17] Dehghani B, Faramarzi L. Experimental investigations of fracture toughness and crack initiation in marble under different freezing and thermal cyclic loading. Constr Build Mater 2019;220:340–52.
[18] Deng Z, Zhan X, Zeng W, Yang S, Wu J. A degradation model of mode-I fracture toughness of rock under freeze-thaw cycles. Theor Appl Fract Mech 2021;115: 103073.
[19] Ebrahimi R, Hosseini M. Experimental study of effect of number of heating–cooling cycles on mode I and mode II fracture toughness of travertine. Theor Appl Fract Mech 2022;117:103185.
[20] Feng G, Kang Y, Chen F, Liu Y-W, Wang X-C. The influence of temperatures on mixed-mode (I+ II) and mode-II fracture toughness of sandstone. Eng Fract Mech 2018;189:51–63.
[21] Feng Z-j, Qiao M-m, Dong F-k, Yang D, Zhao P. Thermal expansion of triaxially stressed mudstone at elevated temperatures up to 400 C. Adv Mater Sci Eng. 2020a;2020.
[22] Feng Z, Zhang C, Dong F, Yang D. Elastic modulus evolution of triaxially stressed mudstone at high temperature up to 400° C. Energy Sci Engng 2020;8: 4126–35.
[23] Fossum A, Freund L. Nonuniformly moving shear crack model of a shallow focus earthquake mechanism. J Geophys Res 1975;80:3343–7.
[24] Freund LB. Dynamic fracture mechanics. Cambridge University Press; 1998.
[25] Funatsu T, Seto M, Shimada H, Matsui K, Kuruppu M. Combined effects of increasing temperature and confining pressure on the fracture toughness of clay bearing rocks. Int J Rock Mech Min 2004;41:927–38.
[26] Ghanbari N, Hosseini M, Saghafiyazdi M. Effects of temperature and confining pressure on the mode I and mode II fracture toughness of cement mortar. Theor Appl Fract Mech 2019;104:102361.
[27] Houhou R, Sutman M, Sadek S, Laloui L. Microstructure observations in compacted clays subjected to thermal loading. Eng Geol 2021;287:105928.
[28] Jiang Y, Zhu Z, Yu L, Zhou L, Zhang R, Ma L. Investigation of the fracture characteristics of granite and green sandstone under different thermal treatments. Theor Appl Fract Mech 2022;118:103217.
[29] Kang P, Hong L, Fazhi Y, Quanle Z, Xiao S, Zhaopeng L. Effects of temperature on mechanical properties of granite under different fracture modes. Eng Fract Mech 2020;226:106838.
[30] Li C, Hu Y, Meng T, Zhang C, Gao R, Jin P, et al. Mode-I fracture toughness and mechanisms of salt-rock gypsum interlayers under real-time high-temperature conditions. Eng Fract Mech 2020;240:107357.
[31] Liu B, Zhu Z, Liu R, Zhou L, Wan D. Study on the Fracture Behavior of Cracks Emanating from Tunnel Spandrel under Blasting Loads by Using TMCSC Specimens. Shock Vib. 2019;2019.
[32] Liu R, Zhu Z, Li Y, Liu B, Wan D, Li M. Study of rock dynamic fracture toughness and crack propagation parameters of four brittle materials under blasting. Eng Fract Mech 2020;225:106460.
[33] Meng T, Guangwu X, Jiwei M, Yang Y, Liu W, Zhang J, et al. Mixed mode fracture tests and inversion of FPZ at crack tip of overlying strata in underground coal gasification combustion cavity under real-time high temperature condition. Eng Fract Mech 2020;239:107298.
[34] Monsif M, Zerouale A, Kandri NI, Mozzon M, Sgarbossa P, Zorzi F, et al. Chemical-physical and mineralogical characterization of ceramic raw materials from Moroccan northern regions: Intriguing resources for industrial applications. Appl Clay Sci 2019;182:105274.
[35] Su H, Qin X, Feng Y, Yu L, Sun Z. Experimental investigation of mixed mode I-II fracture property of thermally treated granite under dynamic loading. Theor Appl Fract Mech. 2022;103267.
[36] Takahashi K, Arakawa K. Dependence of crack acceleration on the dynamic stress-intensity factor in polymers. Exp Mech 1987;27:195–9.
[37] Towhata I, Kuntiwattanaku P, Seko I, Ohishi K. Volume change of clays induced by heating as observed in consolidation tests. Soils Found 1993;33:170–83.
[38] Trindade MJ, Dias M, Coroado J, Rocha F. Mineralogical transformations of calcareous rich clays with firing: a comparative study between calcite and dolomite rich clays from Algarve, Portugal. Appl Clay Sci 2009;42:345–55.
[39] Tsang C-F, Bernier F, Davies C. Geohydromechanical processes in the Excavation Damaged Zone in crystalline rock, rock salt, and indurated and plastic clays—in the context of radioactive waste disposal. Int J Rock Mech Min 2005;42:109–25.
[40] Wan D, Zhu Z, Liu R, Liu B, Li J. Measuring method of dynamic fracture toughness of mode I crack under blasting using a rectangle specimen with a crack and edge notches. Int J Rock Mech Min 2019;123:104104.
[41] Whittaker BN, Singh RN, Sun G. Rock fracture mechanics. Principles, Design Appl. 1992.
[42] Wu Y, Yin T, Tan X, Zhuang D. Determination of the mixed mode I/II fracture characteristics of heat-treated granite specimens based on the extended finite element method. Eng Fract Mech 2021;252:107818.
[43] Yin T, Bai L, Li X, Li X, Zhang S. Effect of thermal treatment on the mode I fracture toughness of granite under dynamic and static coupling load. Eng Fract Mech 2018;199:143–58.

[44] Yin T, Li X, Xia K, Huang S. Effect of thermal treatment on the dynamic fracture toughness of Laurentian granite. Rock Mech Rock Eng 2012;45:1087–94.
[45] Yin T, Tan X, Wu Y, Yang Z, Li M. Temperature dependences and rate effects on Mode II fracture toughness determined by punch-through shear technique for granite. Theor Appl Fract Mech 2021;114:103029.
[46] Yin T, Wu Y, Wang C, Zhuang D, Wu B. Mixed-mode I+ II tensile fracture analysis of thermally treated granite using straight-through notch Brazilian disc specimens. Eng Fract Mech 2020;234:107111.
[47] Yin T, Zhang S, Li X, Bai L. A numerical estimate method of dynamic fracture initiation toughness of rock under high temperature. Eng Fract Mech 2018;204:87–102.
[48] Yoffe EH. LXXV. The moving griffith crack. Lond Edinb Dubl Phil Mag 1951;42:739–50.
[49] Zhang W, Wang C, Guo T, He J, Zhang L, Chen S, et al. Study on the cracking mechanism of hydraulic and supercritical CO2 fracturing in hot dry rock under thermal stress. Energy 2021;221:119886.
[50] Zhang Z, Yu J, Kou S, Lindqvist P-A. Effects of high temperatures on dynamic rock fracture. Int J Rock Mech Min 2001;38:211–25.
[51] Zuo J-P, Xie H-P, Dai F, Ju Y. Three-point bending test investigation of the fracture behavior of siltstone after thermal treatment. Int J Rock Mech Min 2014;70:133–43.